Fish and Shellfish Immunology 160 (2025) 110202

Contents lists available at ScienceDirect

Fish and Shellfish Immunology

journal homepage: www.elsevier.com/locate/fsi

Full length article

Functional studies and synchrotron FTIR biochemical signatures reveal the potential of protein nanoparticles as a VHS virus vaccine

Rosemary Thwaite [a,b], Núria Benseny-Cases [c,1], Mauricio Rojas-Peña [a,b,1], Verónica Chico [d], Maria Carreras [a,b], Sara Puente-Marin [d], Antonio Villaverde [a,e,f], Luis Perez [d], Maria del Mar Ortega-Villaizan [d], Manel Sabés [c], Nerea Roher [a,b,f,*]

[a] Institute of Biotechnology and Biomedicine (IBB), Universitat Autònoma de Barcelona, Bellaterra, (Cerdanyola del Vallès), 08193, Spain
[b] Department of Cell Biology, Animal Physiology and Immunology, Universitat Autònoma de Barcelona, Bellaterra, Cerdanyola del Vallès), 08193, Spain
[c] ALBA Synchrotron Light Source, Carrer de la Llum 2-26, Cerdanyola del Vallès, Barcelona, 08290, Spain
[d] Instituto de Investigación, Desarrollo e Innovación en Biotecnología Sanitaria de Elche (IDiBE), Universidad Miguel Hernández (UMH), Elche, Spain
[e] Department of Genètica i Microbiologia, Universitat Autònoma de Barcelona, Bellaterra, Cerdanyola del Vallès, 08193, Spain
[f] CIBER de Bioingeniería, Biomateriales y Nanomedicina (CIBER-BBN), Madrid, Spain

ARTICLE INFO

Keywords:
Protein nanoparticles
VHSV
Virus specific antibodies
Vaccine
Synchrotron FTIR

ABSTRACT

As an innovative strategy towards new biomaterials for fish vaccine development, we have generated the C-terminal half of the viral haemorrhagic septicaemia virus (VHSV) G protein as nanostructured bacterial inclusion bodies (IBs). IBs offer a slow release of biologically active, native and native-like proteins from a protective scaffold based on a nontoxic amyloid network. These nanoscale materials are an attractive type of vaccine design for aquaculture, being cheap, scalable and stable *in vivo* without the need for encapsulation, unlike soluble proteins. The bacterial remnants carried in IBs, such as lipopolysaccharide, are safe for fish and act as immunostimulants. Here we tested VHSV-G fragment-based protein nanoparticles in a range of scenarios to ascertain cellular uptake, metabolic changes and immunogenicity. Trout (*Oncorhynchus mykiss*) macrophages, in the first line of defence against infections, uptake the particles, resulting in impacts on global cell biochemical signatures measured by synchrotron FTIR. These changes were similar to those observed using inactivated VHSV virus. In a trout VHSV infection model, fish immunized with the developed nanoparticles raised specific anti-VHSV IgM antibodies, detected by ELISA. Among these, neutralizing antibodies were present, shown by a viral neutralization assay in *Epithelioma Papulosum Cyprini* (EPC) carp cell line. Further, the anti-VHSV IgM antibody titre increased significantly in the vaccinated group post VHSV infection, compared to sham-vaccinated fish. We therefore show that viral proteins, nanostructured as IBs, can elicit specific, functional anti-viral antibodies in fish and also can mimic *in vitro* the metabolic signatures associated to viral stimuli. All together, these data demonstrate the potential of this strategy for vaccine development.

1. Introduction

Vaccine development against viral diseases in farmed fish is a prime concern in aquaculture. The number of commercially available vaccines is low considering the size and diversity of the industry [1]. On the other hand, the emergence of viral diseases has increased through intensive rearing and rapid global expansion [2]. Therefore, there is emphasis on finding practical solutions so that fish, particularly juveniles, can be mass vaccinated in a cost-effective manner. In this context, we have drawn on recent work in biomaterials science for alternative strategies. Bacterial inclusion bodies (IBs) have gained interest as tuneable, functional, non-toxic protein nanoparticles [3] produced in bacteria through green and fully scalable methods, during which the recombinant proteins cluster into the bacterial cells as nanoscale particles. They are

Abbreviations: IBs, Bacterial inclusion bodies; VHSV, viral haemorrhagic septicaemia virus; ELISA, Enzyme linked immunosorbent assay; IgM, immunoglobulin M; iRFP, near-infrared fluorescent protein; FTIR, Fourier Transform InfraRed.

* Corresponding author. Institute of Biotechnology and Biomedicine (IBB), Universitat Autònoma de Barcelona, Bellaterra, Cerdanyola del Vallès, 08193, Spain.
E-mail address: nerea.roher@uab.es (N. Roher).

[1] Equally contributed.

https://doi.org/10.1016/j.fsi.2025.110202
Received 8 November 2024; Received in revised form 10 February 2025; Accepted 12 February 2025
Available online 15 February 2025

biologically active, with a high propensity to cross cell membranes and able to function as slow protein-releasing agents [4]. Embracing this concept, we have organized fish viral proteins as nanosized IBs in an innovative vaccine strategy. The advantages of this approach applied to fish vaccines are diverse. IBs are mechanically stable materials *in vivo* without the need for encapsulation and are cheap and easy to produce in *Escherichia coli* [5]. They could be injected or mixed in the feed, retaining the functionality of the forming proteins across a wide pH and temperature range and after lyophilization, which suggests that the IBs are stable at gastrointestinal pH, allowing the recombinant antigen to be administered orally through feed, reducing handling stress associated with intraperitoneal injection [5,6]. In addition, they carry bacterial remnants as such as lipopolysaccharide, peptidoglycans and nucleic acids as impurities, which are potent immunostimulants for fish [7]. The production of recombinant subunit vaccine as IBs in *E. coli* is easy to perform, with a simple enzymatic and mechanical purification process that minimizes costs and allows for quick and easy scaling. Additionally, IBs remain stable under lyophilization conditions across a wide temperature range, highlighting their potential as a pharmaceutical product with a long shelf life, without the need for thermal protection and with high stability for inclusion in extruded feed.

In this context, we already had produced three fish antigenic viral proteins as IBs and demonstrated their uptake *in vitro* in zebrafish liver cells and *in vivo* by zebrafish [8]. In addition, we have shown the innate anti-viral immune response they elicit in zebrafish liver cell line and in trout HKM [8]. In the present study we focus on VHSV-G-frg16^{NP}, namely a vaccine preparation based on nanoparticles made of a fragment of the glycoprotein G of viral haemorrhagic septicaemia virus (VHSV). Viral haemorrhagic septicaemia (VHS) continues to be listed by the World Organization for Animal Health (WOAH) as a notifiable fish disease, demonstrating its global impact and the need for containment (https://www.oie.int/en/animal-health-in-the-world/oie-listed-diseases-2020). The rhabdovirus VHSV causes outbreaks in both freshwater and marine fish including farmed rainbow trout [9], turbot [10], olive flounder [11] and wild fish such as Pacific herring [12]. There are four genotypes related to geographic origin but increasingly, more fish species are being infected [13]. To date there is no commercial vaccine available. The glycoprotein G of VHSV, which protrudes from the virus surface, is the most immunogenic protein of the virus and experimental DNA vaccines encoding it have shown high levels of protection [13,14]. A recent innovation to improve further DNA vaccines is the use of molecular adjuvants. In this strategy, plasmid-encoded signalling molecules are incorporated into a DNA vaccine-adjuvant construct to enhance anti-viral or inflammatory responses [15]. Nevertheless, DNA vaccines face major hurdles to be authorized for marketing due to safety concerns [16]. Alternatives are being sought, such as delivering inactivated virus via mucosal routes [17].

A crucial step in novel vaccine development is the availability of indicators of protection such as ELISA, but also good markers of vaccine action on the immune system. Recently, metabolic reprogramming has been recognized as an important player of defence response to bacterial and viral infection [17,18]. The induction of innate immune responses requires significant metabolic resources, including energy, enzymes and intermediates of macromolecular biosynthesis (e.g., transcription and translation). A viral infection reprograms host metabolism and causes metabolic dysfunction and in parallel, the host implements metabolic changes to mount an effective antiviral response [17,19,20]. In this context and as a proof-of-concept study, we have also explored how to assess global metabolic changes along the pipeline of vaccine development by combining different methodologies to determine how a vaccine works at the cellular and molecular level, and to test vaccine performance. We used in-cell approaches based on conventional cytometry plus confocal microscopy and a global approach using synchrotron-FTIR (μFTIR). μFTIR allows robust global metabolic profiling of cells giving clues about key metabolic changes associated with the immune response after vaccination. In addition, traditional immune indicators such serum ELISA and a viral neutralization assay demonstrated the capacity of VHSV-G-frg16^{NP} to induce specific antibodies against VHSV *in vivo* in a small-scale trout infection model.

2. Materials and methods

2.1. Fish

For the preparation of macrophage primary cultures, rainbow trout (*Oncorhynchus mykiss*) were purchased from a commercial fish supplier (Molinou S.L) and maintained in the Universitat Autònoma de Barcelona (UAB) fish facilities in tanks at 16 °C with a recirculating water system, light/dark regime of 12/12 h and fed daily with a commercial diet. For VHSV infection rainbow trout (*O. mykiss*) juveniles purchased from a VHSV-free commercial fish supplier (Piszolla S.L., Cimballa Fish Farm, Zaragoza, Spain) were maintained in tanks at 14 °C with a recirculating dechlorinated water system, light/dark regime of 12/12 h in the animal facility of the University Miguel Hernandez (UMH). The number of animals used in challenge experiment was approved by the Animal Welfare and the Research Ethics Committee of the Miguel Hernandez University as a pilot scale experiment. Fish were fed daily a commercial diet of approximately 1 % body weight and were acclimatized for 2 weeks prior to the experiment. Mean fish weight 2.2 ± 0.6 g and length 6.0 ± 0.6 cm.

2.2. Nanoparticles

The protein nanoparticle construct, VHSV-G-frg16^{NP}, contains the C-terminal half (amino acid residues 252–450) of the VHSV (07–71) G protein sequence (NCBI Genbank X59148) to the 3′-end, with the Cys residues mutated to Ser to assist expression in *E. coli*. The VHSV clone fragment 16 was originally described in Encinas et al. [21]. Production as bacterial IBs, physical characterization and the innate anti-viral immune response to the nanoparticle *in vitro* are reported elsewhere [8]. The red fluorescent protein (iRFP^{NP}) cloned into pET22b (GeneArt) and transformed into *E. coli* BL21 was used as a non-immune relevant control protein. Both, iRFP^{NP} and VHSV-G-frg16^{NP} were purified using the same protocol.

2.3. Cell culture

Rainbow trout head kidney macrophages (RT-HKM) were isolated from *O. mykiss* (approx. 120 g body weight) following previously described procedures [22]. Primary adherent cultures were established in DMEM + GlutaMAX, 10 % heat-inactivated FBS and 100 μg/ml Primocin (Invitrogen) at 16 °C and 5 % CO_2. Zebrafish ZFL cells (CRL-2643, ATCC) were cultured according to a previously described method [8] at 28 °C and 5 % CO_2 in DMEM + GlutaMAX (Gibco), 10 % heat-inactivated fetal bovine serum (FBS) (Gibco), 0.01 mg/ml insulin (Sigma-Aldrich), 50 ng/ml epidermal growth factor (Sigma-Aldrich), 2 % (v/v) antibiotic/antimycotic (Gibco), and 0.5 % (v/v) trout serum which had been filtered (0.20-μm filter Corning) and heat inactivated for 30 min at 45 °C. Experiments for NP uptake and synchrotron FTIR were performed on day 5 when the macrophages were fully differentiated and at 80 % confluence for the zebrafish ZFL cells.

2.4. Synchrotron FTIR data acquisition and spectra analysis

Macrophages or ZFL were seeded on sterile CaF_2 windows placed in 6-well plates. VHSV-G-frg16^{NP} (10 and 20 μg/ml), iRFP control (20 μg/ml), inactivated VHSV virus (5×10^5 TCID/ml) or Poly I:C (10 μg/ml) were added to cell cultures at 80 % confluence after 2 h incubation in minimal media (without FBS) at 16 and 32 h. After treatment, windows were washed twice with PBS, fixed with paraformaldehyde (1.5 %) for 15 min and dipped three times in doubly distilled water. Windows were air dried for at least 12 h, placed in sealed bags under N_2 atmosphere and

stored at −80 °C until use. FTIR was performed at the MIRAS beamline at ALBA synchrotron (Spain) [23], using a Hyperion 3000 Microscope that was equipped with a 36 × magnification objective coupled to a Vertex 70 spectrometer (Bruker) as described in Benseny-Cases et al. [24].

Spectra of at least 50 cells per condition were acquired with an optical window of 10x10 aperture and analyzed using Opus 7.5 software (Bruker). The spectra exhibiting a low signal-to-noise ratio or high Mie scattering were eliminated. Resonant Mie scattering (RMieS) correction was carried out using the software freely provided online by Peter Gardner's laboratory at the University of Manchester implemented in Matlab, involving 10 iterations in the range of 3100−1300 cm^{-1} and using a scattering particle diameter of 2–8 μm. The effect of the RMieS correction on the entire set of spectra is illustrated in Fig. 2a and b. Ratios were calculated over the following peaks of interest: 1740 cm^{-1} for ν(C=O) (carbonyl) (noted as A_{1740}), 2920 cm^{-1} for CH_2 asymmetric stretching vibrations (noted as A_{2920}), and 1635 cm^{-1} for β-sheet structures (noted as A_{1635}), 1656 cm^{-1} for α-helix structure (noted as A_{1656}) as it has been described in Benseny-Cases et al. [24].

2.5. Uptake of nanostructured viral antigens by macrophages

To test cellular uptake, fluorescently labelled NPs were added to RT-HKM cultures at 70 % confluence after 2–3 h incubation in minimal media (0–0.5 % FBS), at the doses and times indicated below. HK is the main hematopoietic organ in fish and the main source of monocytes/macrophages which have a very well characterised antiviral response *in vitro* [8,25]. For dose–response assays, either 10 or 20 μg/ml VHSV-G-frg16^{NP} were added and cultures were then incubated O/N (16 h). Post treatment, cells were washed in PBS and incubated at 18 °C with 1 mg/ml Trypsin (Gibco) for 15 min. This strong trypsinization step aimed to remove NPs attached to the cell surface [26]. Then, two volumes of complete medium were added, and cells were collected by centrifugation at 300×*g* for 5 min. Pellets were resuspended in PBS for flow cytometry (FACSCalibur BD), and 10,000 events were counted. Data were analyzed using Flowing Software 2.5.1 (University of Turku, Finland) and plotted with Prism 8.01 (GraphPad). A one-way ANOVA was performed with Dunnett's multiple comparisons test, comparing treatment and control means. To confirm that fluorescent NPs were inside the cells, we performed confocal microscopy (Leica). RT-HKM cells were seeded on glass coverslides. The next day, cells at approximately 60 % confluence were placed in minimal media. VHSV-G-frg16^{NP} at 10 and 20 μg/ml were added 2 h later and cells were incubated for 16 h at 18 °C. RT-HKM were fixed with 1.5 % PFA for 15 min at room temperature (RT) and washed with PBS. The cells were stained with DAPI (nuclei) and Cell mask Deep Red (membrane) (Life Technologies). Images were analyzed using Imaris software v8.2.1 (Bitplane) and Fiji (ImageJ 2.0.0, creative commons license).

2.6. RNA extraction and Q-PCR

Total RNA was extracted using TriReagent (Sigma) following the manufacturer's instructions and RNA yield and quality were determined on Nanodrop ND-1000 (Thermo Fisher Scientific) and integrity assessed on the Agilent 2100 Bioanalyzer using RNA 6000 Nano Lab-Chip kit (Agilent Technologies). Then, cDNA was synthesized from 1 μg high quality total RNA using iScript cDNA systhesis kit (Bio-Rad). Quantitative real-time PCR (qPCR) was performed at 60 °C annealing temperature using iTaq Universal SYBR Green Supermix (Bio-Rad) with 250 nM of primers and 2.5 μl of cDNA previously diluted. Each PCR mixture consisted of 5 μl SYBR green supermix, 0.4 μM specific primers, 2 μl diluted cDNA and 2.6 μl water (Sigma-Aldrich) in a final volume of 10 μl. The gene used as reference was *ef1*-α (cDNA diluted to 1:500). The dilution factor for the other tested genes was 1:50 (*vig1*, *mx*, and *ccl4*) or 1:25 (*ifit5* and *mda5*). QPCR Ct were corrected for the dilution factor (Correction Factor = log2 (dilution factor)). All the samples (N = 4 per treatment) were run in triplicate, and data analyzed for individual replicates using the Livak method [27]. Statistical analysis used a one-way unpaired *t*-test to compare each gene's mean fold change in expression with control, using Welch's correction for unequal variances (Prism 8.01, GraphPad) and with $p < 0.05$ considered statistically significant.

2.7. Immunization and blood collection

Fish were anaesthetized in Tricaine (Sigma) 40 mg/l. Using insulin needles (BD microfine 0.3 ml, 30G, BD Biosciences), fish were i.p. injected with 50 μg of VHSV-G-frg16^{NP} or 50 μg of control nanoparticle iRFP^{NP} in a total volume of 30 μl phosphate buffered saline (PBS). Group/tank distribution was as follows: Two tanks for infection: A) iRFP^{NP}, n = 10 fish; B) VHSV-G-frg16^{NP}, n = 12. Two other tanks C) VHSV-G-frg16^{NP}, n = 8 (for blood sampling pre-infection), D) sentinel fish, n = 15 (5 fish for blood sampling pre-infection as untreated control sera, 10 fish as sentinels for survival without any treatment). Fish were then maintained for 30 days and were monitored for well-being and survival as an indicator of macro-toxicity of the nanoparticle. On day 30 post vaccination, fish from the 2 groups designated for blood sampling pre-infection were euthanized by Tricaine overdose (300 mg/l) and blood was taken from the caudal vein with a 26G needle (BD Biosciences). Samples were stored at 4 °C to clot overnight (O/N), centrifuged at 3000×*g* for 15 min at 4 °C and serum was collected and stored at −80 °C.

2.8. VHSV challenge

On day 31 post immunization, fish in the 2 tanks designated for infection (iRFP vaccinated, and VHSV-G-frg16^{NP} vaccinated) were i.p. injected with 30 μl of 3×10^7 median tissue culture infectious dose ($TCID_{50}$)/ml of VHSV-07.71 [28], propagated in EPC (*Epithelioma Papulosum Cyprini*) epithelial carp cell line according to Chico et al. [14], which was isolated in 1969 from skin of a fathead minnow (Winton et al. [29]). Mortality was monitored until 23 days post infection (dpi), when remaining fish were euthanized and blood samples were taken as described above, to collect serum from infection survivors for enzyme linked immunosorbent assay (ELISA).

2.9. Inactivation and concentration of VHSV

To obtain UV-inactivated VHSV to coat ELISA plates, 40 ml of supernatant with VHSV titre 3.16×10^7 $TCID_{50}$/ml was exposed to UV-B at 1 J/cm2 using a Bio-Link Crosslinker BLX E312 (Vilber Lourmat, BLX-E312), as previously described (Garcia-Valtanen et al. [30]) and stored at −80 °C. Virus was concentrated by ultracentrifugation (Sorvall Discovery SE) using a Beckman 70Ti rotor at 35,000 rpm (125,000 g) for 1 h at 4 °C. The pellet was suspended in 500 μl of Sigma water, semi-quantified by spectrophotometry at 280 nm (Nanodrop 1000) and stored at −80 °C.

2.10. IgM antibody response (ELISAs)

To detect the presence of specific antibodies raised against VHSV in the trout sera, from immunized and control fish, both pre and post challenge, we performed indirect ELISAs. Pre-challenge samples were from VHSV-G-frg16^{NP}-vaccinated and untreated fish, and post-challenge samples were from survivors of VHSV-G-frg16^{NP}-vaccinated and iRFP^{NP}-vaccinated fish at the endpoint. Briefly, Maxisorp 96 microwell plates (Nunc) were coated with inactivated VHSV at 0.5 μg/well in 50 μl PBS overnight (O/N) at 4 °C. All further steps were done at RT. Washes were performed in triplicate with PBS +0.05 % (v/v) Tween 20, blocking with 3 % skimmed milk in PBS for 2 h. Serum dilutions were prepared with PBS, 0.05 % (v/v) Tween 20, 0.5 % BSA. Serum dilutions were added in duplicate at 100 μl/well and incubated for 2 h. A monoclonal primary

antibody anti-trout IgM was produced and isolated in house from the mouse hybridoma clone 1.14 (DeLuca et al. [31]). The secondary antibody was HRP conjugated goat anti-mouse IgG (Sigma A4416). Detection was via 3,3′5,5′ tetramethylbenzine (TMB) substrate reagent set (BD Biosciences). Absorbance was measured at 450 nm on a spectrophotometer (Victor 3, PerkinElmer). The specific antibody titre was defined as the inverse of the greatest dilution which still gave a positive result.

2.11. VHSV neutralization assay

To determine the neutralizing capacity of the sera in fish vaccinated with VHSV-G-frg16^{NP} prior to challenge vis-a-vis non-vaccinated, a neutralization assay was performed [14]. Briefly, fish serum was complement-inactivated at 45 °C for 30 min. Serum dilutions were incubated for 3 h at 14 °C with virus at multiplicity of infection (MOI) 3 × 10^{-2} in a 1:10 vol ratio, diluted serum:virus. Then 1 % volume of healthy trout serum was added as a source of complement and the mixture was incubated for a further 30 min. The mixture (100 μl/well in triplicate) was used to infect confluent EPC cells in 96 well plates. Non-serum controls were the same virus preparation mixed, incubated and used to infect EPCs as above with i) a strongly neutralizing monoclonal antibody (MAb) 3FIA2 against the VHSV glycoprotein [32], ii) PBS and 1 % volume healthy trout serum and iii) the virus alone. Infected cells were incubated for 2 h at 14 °C, washed with PBS, and then incubation continued for 24 h in fresh culture medium (RPMI + 2 % FBS). Cells were fixed with 4 % formaldehyde (Sigma) and ice cold methanol, followed by an immunostaining focus assay adapted from Ref. [33] using primary antibody MAb 2C9 (Sanz et al. [34]) and secondary antibody GAM-FITC (Sigma 4600042). Viral infection foci were detected on an IN Cell Analyzer 6000 imaging system (GE Healthcare Life Sciences). Images were processed with Fiji open-source image processing package [35].

2.12. Statistics

Graphs and analyses were performed with Prism 8.01 software (GraphPad), except for synchrotron data analysis that were performed as indicated in materials and methods. Data are shown as mean ± standard error of the mean (SEM) and $p < 0.05$ was considered statistically significant.

3. Results and discussion

3.1. Uptake and anti-viral response of primary macrophages treated with VHSV protein nanoparticles (VHSV-G-frg16^{NP})

Following exposure to 20 μg/ml of protein, VHSV-G-frg16^{NP} was rapidly internalized, with around 40 % of HKM cells exhibiting fluorescence after 16 h of incubation (Fig. 1a and b). The internalization dynamics followed a dose-response profile with cells incubated at higher doses showing greater fluorescence levels (Fig. 1a). Internalization of 20 μg/ml VHSV-G-frg16^{NP} was confirmed by confocal microscopy (Fig. 1b), revealing accumulation of nanoparticles in the cytosol, in form of large clusters (Fig. 1b). While some cells engulfed high material amounts, others were poorly fluorescent. Confocal image analysis showed that between 10 and 20 % of VHSV-G-frg16^{NP}-treated cells showed green fluorescence inside the cytosol. This is quite consistent with the cytometry results, in which up to ~40 % of cells were fluorescent, upon O/N exposure to the same dose as in the confocal experiments (20 μg/ml) (Fig. 1b). To determine whether the VHSV-G-frg16^{NP} could elicit an antiviral response in line with that provoked by viral infection, HKM were stimulated with Poly(I:C), two VHSV-G-frg16^{NP} doses and inactivated virus (Fig. 1c). Poly(I:C) and the inactivated virus induced a strong expression of typical anti-viral genes in macrophages such as *vig1*, *mx*, *ifit5*, *mda5* and *ifna* (Fig. 1c). VHSV-G-frg16^{NP}, at 10 and 20 μg/ml, also induced the expression of antiviral markers at lower levels, following a dose-response pattern (Fig. 1c). Rainbow trout is the most susceptible species to VHS virus, and the head kidney is one of its main target organs (WOAH, 2022). HK isolated macrophages can trigger a robust primary antiviral response, including the secretion of cytokines as well as acting as antigen-presenting cells (APCs) when they are exposed to antigenic proteins or viral PAMPs such as Poly(I:C) [8,35]. The VHSV-G-frg16^{NP} could induce an innate antiviral response in line with provoked by inactivated virus that are the most common vaccine form. The differences in gene expression between typical viral stimuli (Poly I:C or inactivated virus) and VHSV-G-frg16^{NP} could be due to the fact that all macrophages in the cell culture could potentially respond to Poly(I:C) or virus, but not all the macrophages internalized and responded to VHSV-G-frg16^{NP} nanoparticles. Only a maximum of 20 % of cells assessed by confocal microscopy and 40 % of cells assessed by cytometry were responding to VHSV-G-frg16^{NP} (Fig. 1a, b and c). Importantly, protein nanoparticles made with an irrelevant immune protein (iRFP) did not induce significant gene expression changes (Fig. 1c). The antiviral responses observed in this study are in line with antiviral expression reported in other vaccine that we already had produced. For example, nanostructured SVCV G3 antigen and SVCV G3 combined with a recombinant zebrafish interferon-gamma (IFNγ) produced in *E. coli*, have been shown to induce a strong antiviral immune response, and *in vivo* the SVCV G3 plus IFNγ was able to protect zebrafish against SVC virus infection [6].

3.2. Synchrotron μFTIR analysis of primary macrophages treated with VHSV and Inactivated VHSV

In order to study the effect of VHSV-G-frg16^{NP} on trout macrophages cells (HKM) we used Fourier transform infrared microscopy (μFTIR) to analyze four different types of samples: untreated control cells, Poly(I:C)-treated cells, inactivated VHS virus-treated cells and VHSV-G-frg16^{NP}-treated cells at two different concentrations, all at two different time points. FTIR spectra in the 3000–800 cm^{-1} region (Fig. 2a) were recorded and corrected for Mie Scattering (Fig. 2b). Optical images of the cells analyzed are shown in Fig. 2c. Second derivative spectra were calculated to enhance the resolution of the absorption bands (Fig. 3). A minimum of 50 single-cell spectra were recorded and compiled for each condition to statistically represent and compare the different treatments. Since FTIR spectroscopy is sensitive to protein aggregation, a β-sheet peak could be observed *in vitro* in the Amide I region (1720-1600 cm^{-1}) for VHSV-G-frg16^{NP} (Fig. 2d) which allows measuring whether VHSV-G-frg16^{NP} has been taken up. Considering that not all the macrophages internalise VHSV-G-frg16^{NP}, the use of FTIR has been shown to be very sensitive in detecting protein intracytoplasmic clusters and thus internalization of VHSV-G-frg16^{NP} (explained below).

μFTIR analysis of macrophages treated with VHSV-G-frg16^{NP} demonstrated a significant increase of carbonyl (ester) groups (measured by calculating the ratio 1740 cm^{-1}/2920 cm^{-1}) indicating an increase in lipid oxidation, to a similar level as macrophages treated with inactivated virus. Also, an increase of β-sheet structures (measured by calculating the ratio 1635 cm^{-1}/1656 cm^{-1}) in the cells treated with VHSV-G-frg16^{NP} at 20 μg/ml after 16 h of the treatment can be observed (Figs. 4 and 5, respectively). No significant changes were found in the amide I and II peaks (protein), in the PO_2 peaks (nucleic acids) (data non shown) or within the carbohydrate peak. Treatment with Poly(I:C) has been extensively used to emulate a viral infection of dsRNA viruses. Poly (I:C) interacts with TLR3 at the endosomal membrane and MDA5 stimulating downstream signalling pathways [36]. The activation of these pathways prepares the cell to fight and clear viruses. Interestingly, changes in the lipid oxidation peaks in the Poly(I:C) treated cells were different from those stimulated by the inactivated virus or the VHSV-G-frg16^{NP} protein nanoparticles. These results probably indicate different underlying mechanisms of cell response depending on the cell receptor [37] and the internalization pathway. Differences between control cells and VHSV-G-frg16^{NP} treated cells are evident at the highest

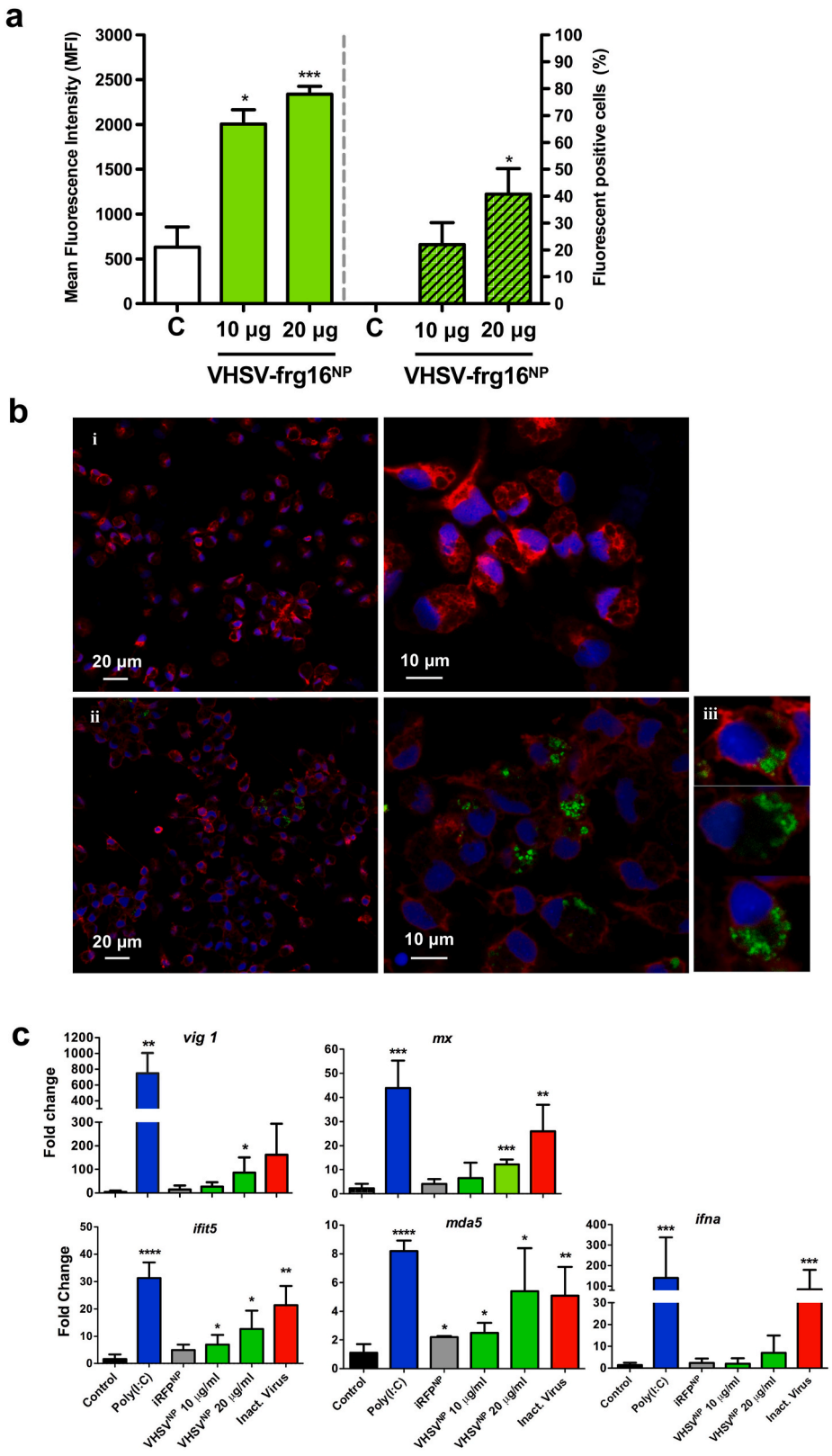

Fig. 1. Uptake of Protein nanoparticle VHSV-G-frg16^{NP} by differentiated macrophages. (a) Fluorescently labelled VHSV-G-frg16^{NP} were added to macrophages, incubated for 16 h with NPs 10–20 µg/ml and uptake evaluated by cytometry. Differences between means were analyzed by a one-way ANOVA with Dunnett's multiple comparisons test, treatments versus control. Significance levels *$p < 0.05$; **$p < 0.01$; ***$p < 0.001$; ****$p < 0.0001$. (b) Confocal microscopy and digitalized image (z-stacks) of macrophages after 16 h incubation with 20 µg/ml VHSV-G-frg16^{NP}. NPs are green, cell membrane red, and nuclei blue. (i) Control confocal image without NPs. (ii) and (iii) representative images of VHSV-G-frg16^{NP} treated macrophages. (c) *vig1*, *mx*, *ifit5*, *mda5* and *ifna* expression changes in macrophages treated with Poly(I:C) at 10 µg/ml, iRFP at 20 µg/ml, VHSV-G-frg16^{NP} at 10–20 µg/ml and inactivated virus.

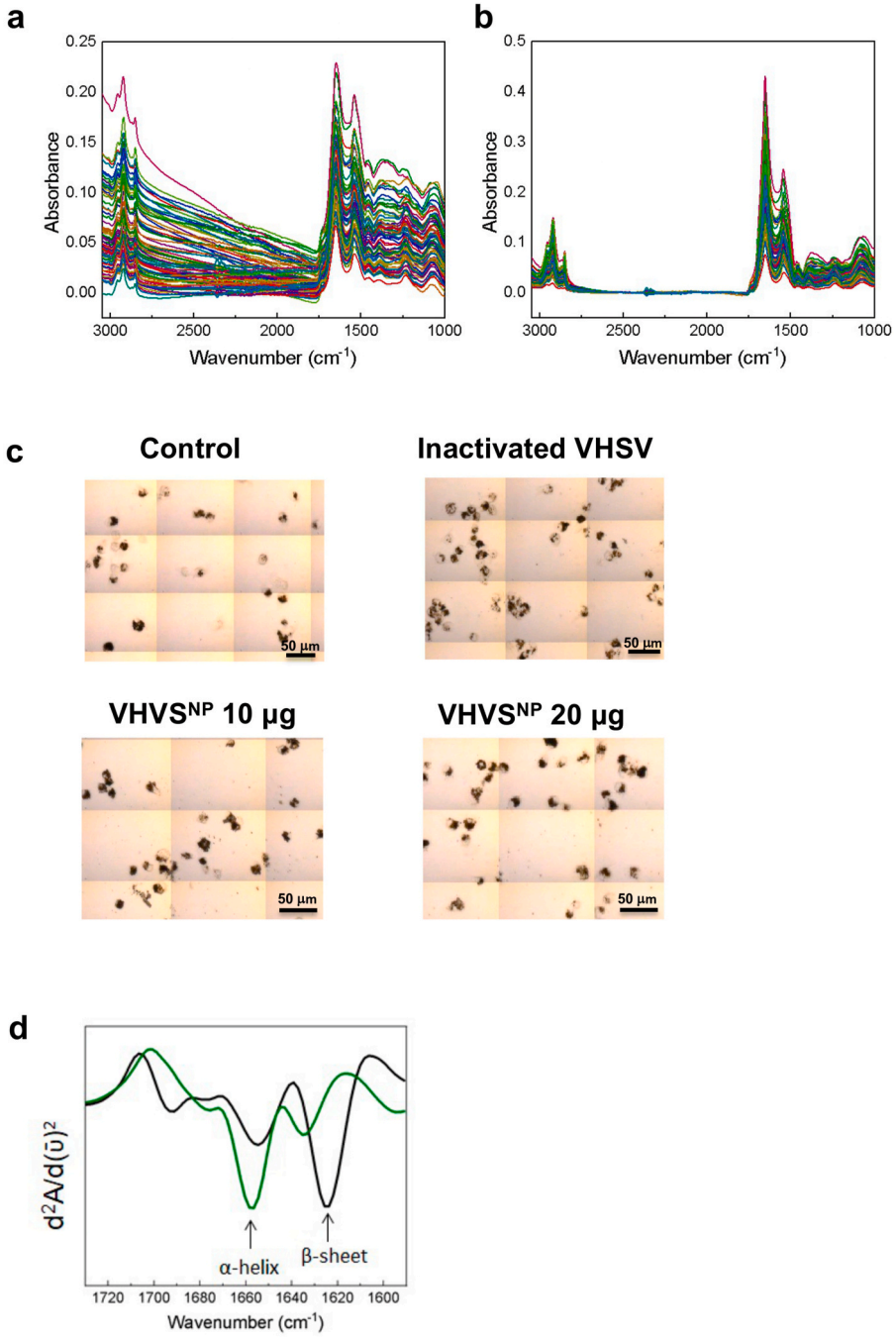

Fig. 2. Data pre-treatment and optical images (a) All spectra for the different experimental conditions studied (b) and the same set of spectra after RMieS correction. (c) Optical images of the trout macrophage with no treatment and treated with Inactivated VHSV and VHSV-G-frg16^{NP} 10 and 20 µg/ml. Scale bar: 50 µm. (d) Second derivative of the Amide I region Infrared spectrum for a non-treated cell (green) and for a VHSV-G-frg16^{NP} *in vitro* (black).

nanoparticle concentration at 16 h and similar to the changes induced by inactivated virus (Fig. 4). Both treatments increased the membrane lipid peroxidation at 16 h while at 32 h the cells are recovering to the initial state (back to homeostasis), thus we observed a decrease in the lipid peroxidation peak. Moreover, similar results were obtained with a zebrafish liver cell line (ZFL) (Supplementary Fig. 1). We observed an increase in lipid peroxidation at 16 h in ZFL cells exposed to VHSV-G-frg16^{NP} at 20 µg/ml, which finally returned to a non-activated state at 32 h. However, zebrafish liver cells do not behave in the same way as macrophages did in response to Poly(I:C). The 1740 cm^{-1}/2920 cm^{-1} ratio indicated an induction of lipid peroxidation by Poly(I:C) at 16 h similar to that induced by VHSV-G-frg16^{NP}. We can conclude that lipid peroxidation was the main effect after VHSV-G-frg16^{NP} and it was similar to that of Inactivated virus. Lipid peroxidation is induced by ROS (reactive oxygen species) and cellular membranes or organelle membranes, due to their high polyunsaturated fatty acids (PUFAs), are especially susceptible to ROS damage. The activation of immune cells requires cell proliferation, which in turn requires the coordinated action of catabolic and anabolic pathways. Thus, ROS generation and lipid peroxidation become part of the antiviral response of immune cells and, VHSV-G-frg16^{NP} mimics the cell response to a virus, leading us to infer that VHSV-G-frg16^{NP} induce a correct metabolic immune response and together with correlates of protection uncovers its potential as a vaccine.

To further investigate the lipid oxidation status after VHSV-G-

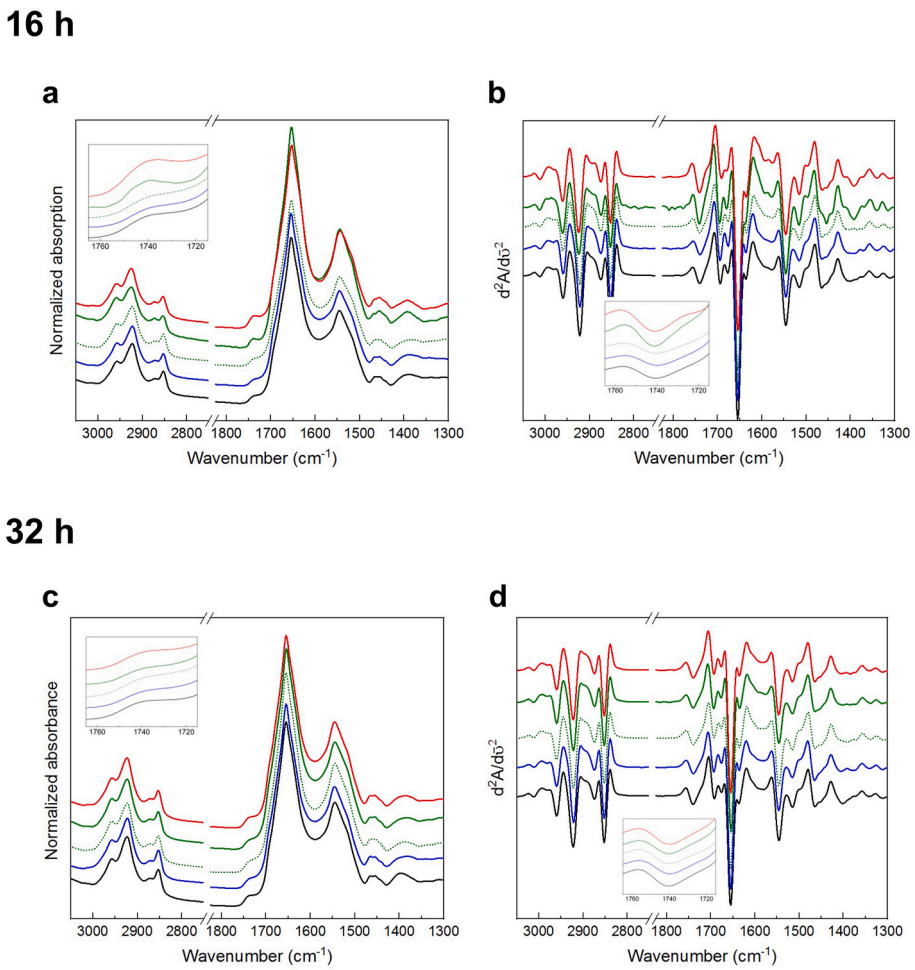

Fig. 3. Average spectra of different conditions (a) Average infrared spectra of each condition at 16 h normalized by the total lipid (band at 2920 cm^{-1}), (b) Second derivative of the average spectra at 16 h, (a) average infrared spectra of each condition at 32 h normalized by the total lipid (band at 2920 cm^{-1}), (b) second derivative of the average spectra at 32 h. The aldehyde band at 1740 cm^{-1} is showed as an inset in all panels. Color code: Control in black, Poly(I:C) in blue, VHSV-G-frg16^{NP} 10 μg in doted green line, VHSV-G-frg16^{NP} 20 μg in green and inactivated virus in red.

frg16^{NP} exposure we measured MDA in HKM cells but we did not observe any significant change in cell peroxidation status at 16 and 32 h at any of the tested conditions (Supplementary Fig. 2). Phospholipids present in cell membranes are mainly polyunsaturated fatty acids (PUFAs), which are especially vulnerable to oxidation. Oxidation of PUFAs produces reactive species such as, acrolein, 4-hydroxy-2-nonenal (4-HNE), 4-oxo-2-nonenal (4-ONE), 4-hydroxy-2-hexanal (4-HHE), 2-hexenal, crotonaldehyde as well as the dialdehydes glyoxal and malondialdehyde (MDA). Quantification of lipid peroxidation in biological samples has been extensively performed with the thiobarbituric acid (TBA) test that detects malondialdehyde (MDA), an end-product PUFA oxidation (Pillon et al. [38]). In our experiments, MDA levels did not increase significantly but we cannot discard that other intermediate metabolites (eg. 4-HNE) would play a more important role in lipid peroxidation in trout macrophages.

3.3. Production of specific anti-VHSV IgM

Trout vaccinated with VHSV-G-frg16^{NP} clearly induced a specific antibody response by 30 days post i.p. immunization, with a pre-challenge titre of 240 (Fig. 6a). Moreover, 23 days post VHSV challenge, a substantial specific antibody expansion was observed with antibodies still detectable at 8 times this dilution (titre 1920). It was not possible to compare antibody expression between fish vaccinated with iRFP^{NP} control vs. fish vaccinated with VHSV-G-frg16^{NP} because 90 % (9/10) of the iRFP-vaccinated fish died (Fig. 6b) before 30 days after i.p. immunisation. However, the survival data showed that VHSV-G-frg16^{NP} was able to confer protection, particularly with respect to the immune irrelevant control iRFP^{NP} (Fig. 6b).Thus, it has been demonstrated here that the protein nanoparticle VHSV-G-frg16^{NP} induces specific antibodies against VHSV in juvenile trout and can protect them against viral infection, without the use of any adjuvant. The ELISA results showed a clear induction of specific antibodies 30 days post immunization, with a large, consistent expansion post-infection. On the other hand, the production of the recombinant VHSV-G-frg16^{NP} is cheap, robust and simple [8]. As a conventional soluble protein, the immunogenicity of VHSV protein G frg16 has been demonstrated by pepscan mapping [39] and by antibody binding studies using sera from VHSV infection survivors [21]. But the novel protein configuration proposed here overcomes the difficulties faced in making labile soluble proteins into viable vaccine formats, without any further need for encapsulation. Here, VHSV-G-frg16^{NP} released enough bioactive native-like protein from within the network of IB amyloid aggregate, to induce *in vivo* specific antibody production. This mechanism of slow release of functional protein by IBs is currently being explored in applications for human medicine [40]. In this work, we show the use of IBs to raise virus-specific antibodies *in vivo* as an antiviral vaccine strategy for fish. Importantly, no sign of macro-toxicity was observed during the 30-day period post immunization with VHSV-G-frg16^{NP} and only 1 death in a total of 20 fish vaccinated was reported while all others showed no signs of malaise.

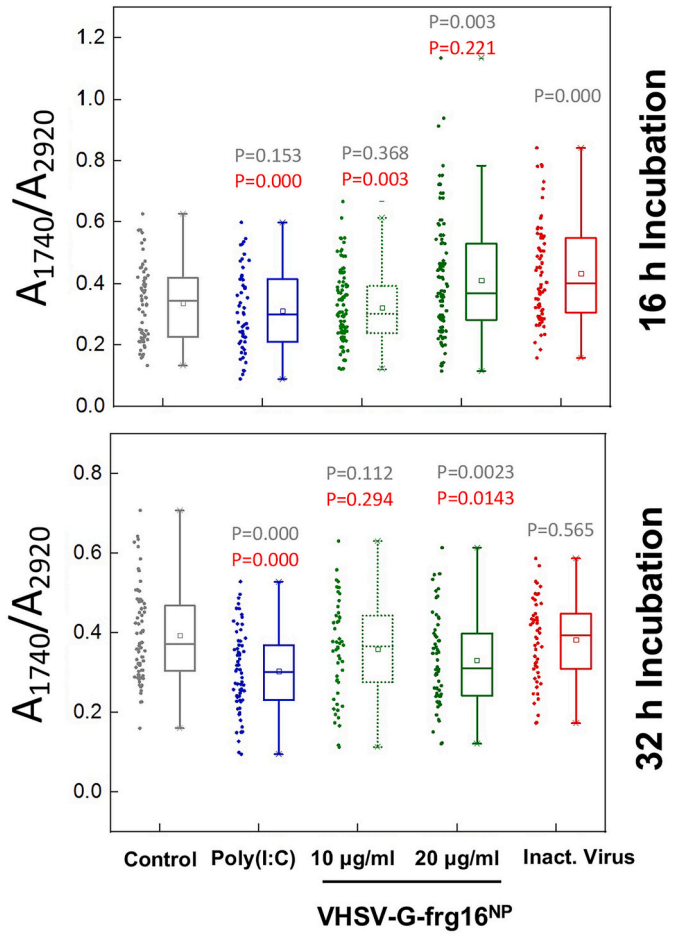

Fig. 4. Lipid oxidation ratio. Box plot of the lipid carbonyl/CH_2 ratio expressed as the ratio of the corresponding absorbance at 1740 cm^{-1} and 2920 cm^{-1} at 16 h (a) and 32 h (b) for the different conditions. P values were calculated by T-test two tailed distribution and two sample equal variance. Color code: Control in gray, Poly(I:C) in blue, VHSV-G-frg16^{NP} 10 µg in doted green line, VHVS^{NP} 20 µg in green and inactivated virus in red. For each condition statistical significance against the Control are shown in gray and statistical significance against the Inactivated virus in red.

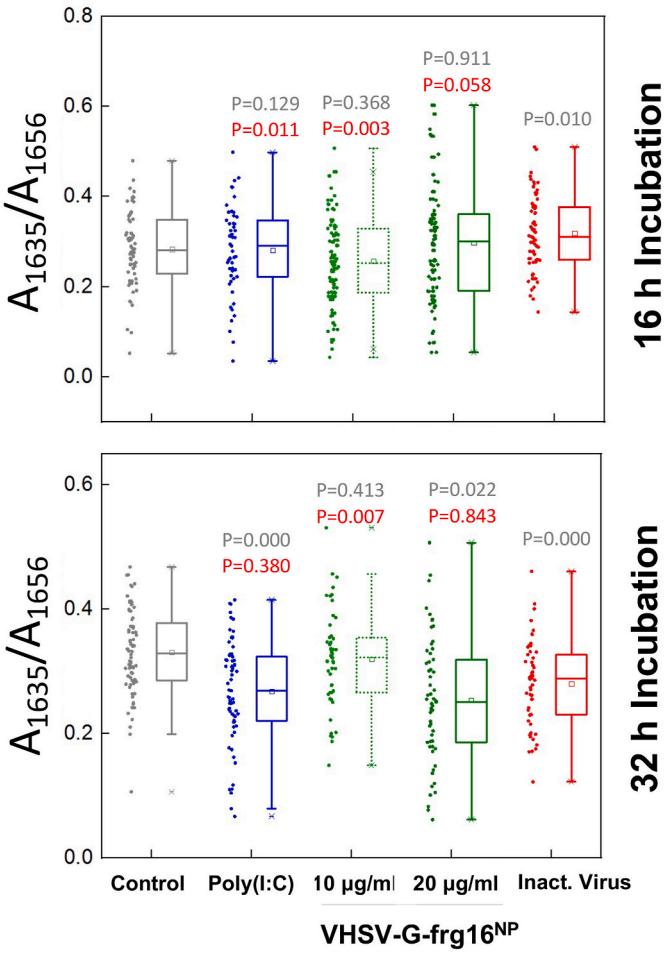

Fig. 5. Protein aggregation ratio. Box plot for the protein aggregation ratio expressed as the ratio for β-sheet structures (1635 cm^{-1}) and α-helix structures (1656 cm^{-1}). P values were calculated by T-test two tailed distribution and two sample equal variance. Colour code is the same than in Fig. 4.

This is in line with our other studies using this and other IBs in zebrafish and sole, in which no detrimental effects have been observed [5,7,34,41]. We therefore consider the nanoparticle safe in terms of macro-toxicity.

3.4. Neutralizing assays

To see if antibodies raised by VHSV-G-frg16^{NP} immunization could inhibit VHSV activity, a neutralization assay was performed. Only the sera of vaccinated fish pre-challenge and untreated controls were used. In this way, neutralizing antibodies, if present, could be directly linked to vaccination. Fig. 7a shows the number of viral foci formed when diluted sera (1:25) were incubated with VHSV. Compared to the control (virus incubated with PBS before adding complement), the sera of VHSV-G-frg16^{NP} vaccinated fish were able to decrease virus infection of the cells significantly, while sera from unvaccinated control fish did not significantly decrease viral infection. There was, however, some overlap between groups, showing a range of neutralizing capacity among individual fish sera and their antibodies. Fig. 7b provides representative examples of the VHSV focus forming units found in treatments with PBS control and sera from VHSV-G-frg16^{NP} vaccinated fish. Not only there were less focus forming units when the virus was incubated with sera from VHSV-G-frg16^{NP} vaccinated fish, but also very large foci were primarily found in the PBS control and the unvaccinated control groups, as well as in the virus only technical control. This indicates more viral propagation in the control groups. The overlap observed in the neutralizing activity of certain serum samples of unvaccinated and vaccinated fish ($p = 0.0845$) is likely due to natural antibodies (Fig. 7a). Interestingly, fish, as other vertebrates, have natural antibodies that are present without apparent antigenic stimulation and in trout they can partially neutralize VHSV [42]. However, the number of focus forming units per ml for virus mixed with the sera of VHSV-G-frg16^{NP} vaccinated fish, was significantly different from that of virus mixed with the sera of iRFP^{NP} vaccinated fish, which could explain the high mortality observed in the survival curve of fish vaccinated with the immune irrelevant control iRFP^{NP}. Concerning immunogenicity, it is of interest for vaccine design that VHSV-G-frg16^{NP}-induced antibodies showed virus neutralizing capacity, despite having Cys mutated to Ser in order to facilitate production in *E. coli*. Note that Cys on the protein surface are one of the three signature amino acids for antigenic determinants [43] and are strongly implicated in the tertiary structure. Inhibition of VHSV infectivity by a similar assay to that conducted here has been reported using fish sera vaccinated with a DNA vaccine encoding the G protein and 2-4 added CpG motifs [44]. Being this is a small scale, but crucial, proof of concept study, optimization of dose, immunization regime, the challenge model and exploration of alternative delivery routes is work for the future. We show in trout juveniles, VHSV-G-frg16^{NP} induces the production of specific anti-VHSV antibodies which are functional against VHSV, as a surrogate of protection. The work here demonstrates

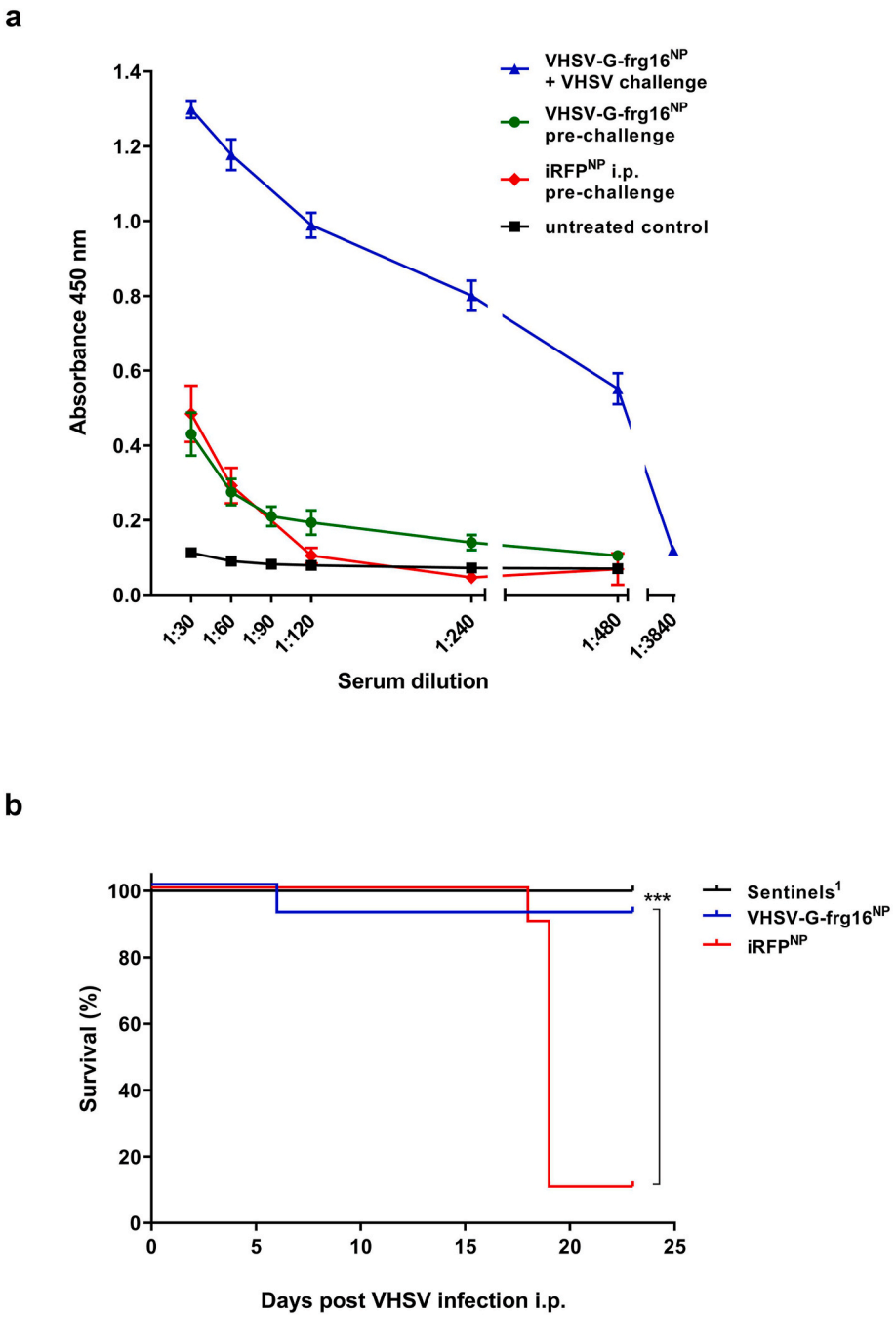

Fig. 6. Presence of specific anti-VHSV IgM in sera and survival curve of rainbow trout juveniles immunized with protein nanoparticle VHSV-G-frg16^{NP}, challenged with VHSV. (a) ELISA titration curves using inactivated VHSV as antigen. Trout were vaccinated i.p. with 50 μg VHSV-G-frg16^{NP} or 30 μl PBS and left for 30 days until VHSV challenge. Sera for ELISA collected from: untreated control (■); VHSV-G-frg16^{NP} vaccinated pre-challenge (●); iRFP^{NP} vaccinated pre-challenge (♦); VHSV-G-frg16^{NP} vaccinated and challenged with VHSV, infection survivors at 23 dpi (▲). Absorbance readings were measured at 450 nm. Error bars indicate standard error of the mean (SEM), n = 4. dpi = days post infection. (b) Fingerling trout of 30 days after i.p. injection with: 50 μg VHSV-G-frg16^{NP} (n = 12) (blue) or 50 μg iRFP^{NP} control (n = 10) (Red) were challenged with i.p. injection of 30 μl of 3×10^7 TCID50/ml viral haemorrhagic septicaemia virus (VHSV). [1]Untreated and not challenged control fish. Significant differences were analyzed using the Log-rank test ***, $p < 0.001$. Sentinels were untreated, uninfected controls (**black**).

the *in vivo* potential of IBs, made of antigenic viral proteins, as a viable, practical biomaterial for the development of novel vaccines in aquaculture.

4. Conclusions

In line with the search of new antiviral vaccines for aquatic organisms we have developed a protein-made biomaterial designed to have immune specificity, potency and improved resistance to gastrointestinal and aquatic conditions. It could therefore be injected or orally administrated. We have demonstrated that the VHSV-G-frg16^{NP} protein nanoparticles are biocompatible, are taken up by macrophages and induce a variety of cellular and molecular changes similar to those induced by inactivated virus, the most common format of viral vaccines. These changes correlated with *in vivo* systemic responses:immunoglobulin titre and antibody neutralizing activity.This proof-of-concept trial allows us to propose VHSV-G-frg16^{NP} as a new generation platform for VHSV vaccination.

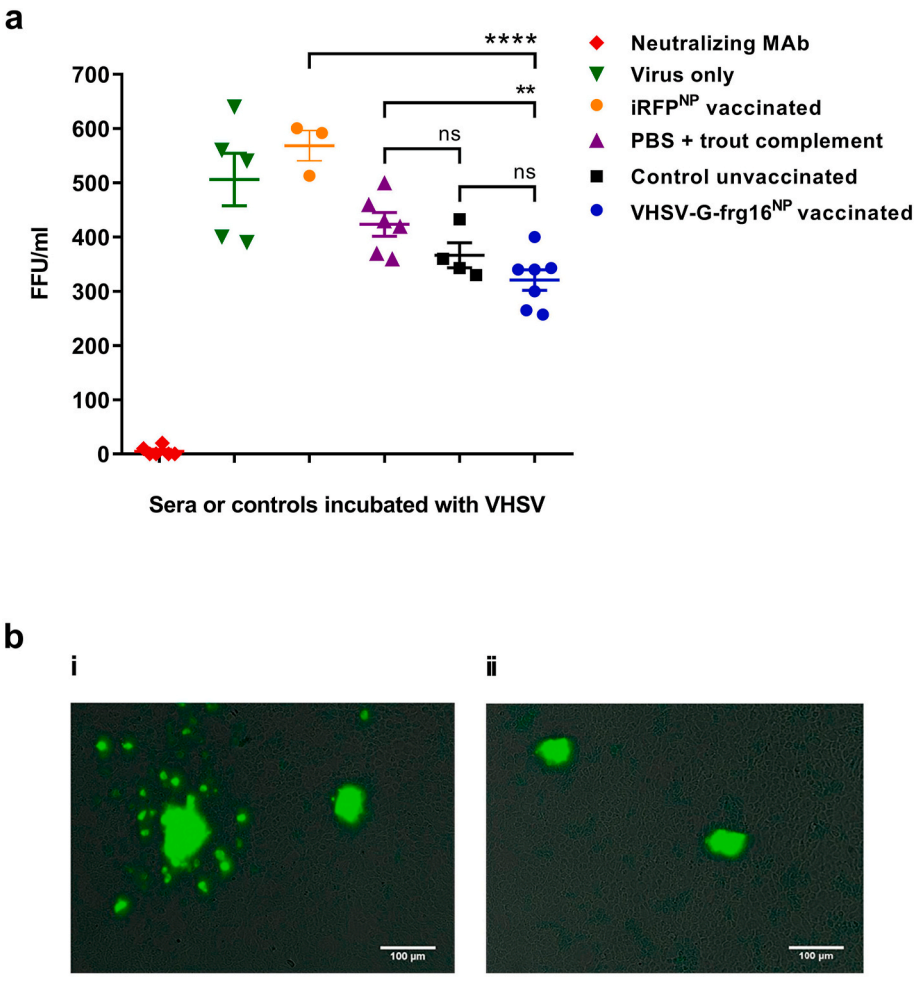

Fig. 7. Neutralizing capacity of sera in juvenile trout 30 days post immunization with protein nanoparticle VHSV-G-frg16^{NP}. (a) Neutralization assay quantified by viral focus forming units (FFU) detected using an immunostaining focus assay. Graph shows FFU/ml using virus mixed with sera diluted at 1:25 from VHSV-G-frg16^{NP} vaccinated (●), and unvaccinated control fish (■), compared to virus mixed with PBS and complement (▲) and iRFP^{NP} control vaccinated (●) in parallel. Error bars indicate standard error of the mean (SEM), minimum n = 3 fish. Horizontal bar = mean. Statistical analysis was a one-way ANOVA with Dunnett's multiple comparisons test against the PBS + complement control group. Significance level **p < 0.01; ****$p < 0.001$; ***$p < 0.0001$, ns = not significant. Technical experimental controls were virus mixed with neutralizing MAb (♦), and virus alone (▼). (b) Representative images of viral FFU in treatment groups described in Fig. 7a. Images are merged brightfield and FITC. (i) PBS + complement control (ii) VHSV-G-frg16^{NP} vaccinated.

CRediT authorship contribution statement

Rosemary Thwaite: performed experiments, designed experiments, analyzed data, wrote the manuscript. **Núria Benseny-Cases:** performed experiments, analyzed data, wrote the manuscript. **Mauricio Rojas-Peña:** performed experiments. **Verónica Chico:** designed experiments. **Maria Carreras:** performed experiments. **Sara Puente-Marin:** performed experiments. **Manel Sabés:** oversaw the research. **Antonio Villaverde:** oversaw the research. **Luis Perez:** oversaw the research. **Maria del Mar Ortega-Villaizan:** oversaw the research. **Nerea Roher:** designed experiments, wrote the manuscript, conceived ideas, oversaw the research, All authors were involved in discussions and contributed to the final writing of the manuscript.

Ethics statement

All methods were performed in accordance with the Spanish and European regulations (RD53/2013 and EU Directive 2010/63/EU) for the protection of animals used for research experimentation and other scientific purposes.

Funding

This work was supported by grants from the Spanish Ministry of Science, European commission and AGAUR funds to NR (AGL2015-65129-R MINECO/FEDER, RTI2018-096957-B-C21 MINECO/FEDER and 2014SGR-345 AGAUR). The European Research Council fund to MOV (ERC Starting Grant GA639249). RT was supported by a pre-doctoral scholarship from AGAUR (Spain).

Declaration of competing interest

The authors declare that the research was performed without any conflict of interest.

Acknowledgements

We thank Efren Lucas and Remedios Torres for technical assistance. These experiments were performed at MIRAS beamline at ALBA Synchrotron with the collaboration of ALBA staff.

Appendix A. Supplementary data

Supplementary data to this article can be found online at https://doi.org/10.1016/j.fsi.2025.110202.

Data availability

Data will be made available on request.

References

[1] A.K. Dhar, S.K. Manna, F.C. Thomas Allnutt, Viral Vaccines for Farmed Finfish, Jan. 2014, https://doi.org/10.1007/s13337-013-0186-4.

[2] F.S. Kibenge, Emerging Viruses in Aquaculture, Elsevier B.V., Feb. 01, 2019, https://doi.org/10.1016/j.coviro.2018.12.008.

[3] E. García-Fruitós, et al., Bacterial inclusion bodies: making gold from waste, Trends Biotechnol. 30 (2) (Feb. 2012) 65–70, https://doi.org/10.1016/j.tibtech.2011.09.003.

[4] U. Rinas, E. Garcia-Fruitós, J.L. Corchero, E. Vázquez, J. Seras-Franzoso, A. Villaverde, Bacterial inclusion bodies: discovering their better half, Trends Biochem. Sci. 42 (9) (Sep. 2017) 726–737, https://doi.org/10.1016/j.tibs.2017.01.005.

[5] D. Torrealba, et al., Nanostructured recombinant cytokines: a highly stable alternative to short-lived prophylactics, Biomaterials 107 (Nov. 2016) 102–114, https://doi.org/10.1016/j.biomaterials.2016.08.043.

[6] M. Rojas-Peña, et al., How modular protein nanoparticles may expand the ability of subunit anti-viral vaccines: the spring viremia carp virus (SVCV) case, Fish Shellfish Immunol. 131 (Dec. 2022) 1051–1062, https://doi.org/10.1016/J.FSI.2022.10.067.

[7] A. Ruyra, et al., Targeting and stimulation of the zebrafish (Danio rerio) innate immune system with LPS/dsRNA-loaded nanoliposomes, Vaccine 32 (31) (Jun. 2014) 3955–3962, https://doi.org/10.1016/j.vaccine.2014.05.010.

[8] R. Thwaite, et al., Protein nanoparticles made of recombinant viral antigens: a promising biomaterial for oral delivery of fish prophylactics, Front. Immunol. 9 (Jul) (2018), https://doi.org/10.3389/fimmu.2018.01652.

[9] M. Raja-Halli, et al., Viral haemorrhagic septicaemia (VHS) outbreaks in Finnish rainbow trout farms, Dis. Aquat. Org. 72 (Oct. 2006) 201–211, https://doi.org/10.3354/dao072201.

[10] P. Pereiro, A. Figueras, B. Novoa, Turbot (Scophthalmus maximus) vs. VHSV (viral hemorrhagic septicemia virus): a review, Front. Physiol. 7 (May 2016), https://doi.org/10.3389/fphys.2016.00192.

[11] W.-S. Kim, et al., An outbreak of VHSV (viral hemorrhagic septicemia virus) infection in farmed olive flounder Paralichthys olivaceus in Korea, Aquaculture 296 (1–2) (Nov. 2009) 165–168, https://doi.org/10.1016/j.aquaculture.2009.07.019.

[12] J. Lovy, N.L. Lewis, P.K. Hershberger, W. Bennett, T.R. Meyers, K.A. Garver, Viral tropism and pathology associated with viral hemorrhagic septicemia in larval and juvenile Pacific herring, Vet. Microbiol. 161 (1–2) (Dec. 2012) 66–76, https://doi.org/10.1016/j.vetmic.2012.07.020.

[13] H.F. Skall, N.J. Olesen, S. Mellergaard, Viral haemorrhagic septicaemia virus in marine fish and its implications for fish farming – a review, J. Fish. Dis. 28 (9) (Sep. 2005) 509–529, https://doi.org/10.1111/j.1365-2761.2005.00654.x.

[14] V. Chico, et al., The immunogenicity of viral haemorragic septicaemia rhabdovirus (VHSV) DNA vaccines can depend on plasmid regulatory sequences, Vaccine 27 (13) (Mar. 2009) 1938–1948, https://doi.org/10.1016/j.vaccine.2009.01.103.

[15] J.M.S. Lazarte, et al., Enhancement of glycoprotein-based DNA vaccine for viral hemorrhagic septicemia virus (VHSV) via addition of the molecular adjuvant, DDX41, Fish Shellfish Immunol. 62 (Mar. 2017) 356–365, https://doi.org/10.1016/j.fsi.2017.01.031.

[16] C. Collins, N. Lorenzen, B. Collet, DNA vaccination for finfish aquaculture, Fish Shellfish Immunol. 85 (Feb. 2019) 106–125, https://doi.org/10.1016/j.fsi.2018.07.012.

[17] S. Kole, S.S.N. Qadiri, S.-M. Shin, W.-S. Kim, J. Lee, S.-J. Jung, PLGA encapsulated inactivated-viral vaccine: formulation and evaluation of its protective efficacy against viral haemorrhagic septicaemia virus (VHSV) infection in olive flounder (Paralichthys olivaceus) vaccinated by mucosal delivery routes, Vaccine 37 (7) (Feb. 2019) 973–983, https://doi.org/10.1016/j.vaccine.2018.12.063.

[18] D. Wu, et al., Type 1 interferons induce changes in core metabolism that are critical for immune function, Immunity 44 (6) (Jun. 2016) 1325–1336, https://doi.org/10.1016/J.IMMUNI.2016.06.006.

[19] J. Van den Bossche, L.A. O'Neill, D. Menon, Macrophage immunometabolism: where are we (going)? Trends Immunol. 38 (6) (Jun. 2017) 395–406, https://doi.org/10.1016/J.IT.2017.03.001.

[20] S. Zhang, J. Carriere, X. Lin, N. Xie, P. Feng, Interplay between cellular metabolism and cytokine responses during viral infection, Viruses 10 (10) (Oct. 2018), https://doi.org/10.3390/V10100521.

[21] P. Encinas, et al., Rainbow trout surviving infections of viral haemorrhagic septicemia virus (VHSV) show lasting antibodies to recombinant G protein fragments, Fish Shellfish Immunol. 30 (3) (Mar. 2011) 929–935, https://doi.org/10.1016/J.FSI.2011.01.021.

[22] N. Roher, A. Callol, J.V. Planas, F.W. Goetz, S.A. MacKenzie, Endotoxin recognition in fish results in inflammatory cytokine secretion not gene expression, Innate Immun. 17 (1) (Feb. 2011) 16–28, https://doi.org/10.1177/1753425909348232.

[23] I. Yousef, et al., MIRAS: the infrared synchrotron radiation beamline at ALBA, Synchrotron Radiat. News 30 (4) (Jul. 2017) 4–6, https://doi.org/10.1080/08940886.2017.1338410/ASSET//CMS/ASSET/F1125EE4-565E-492E-BB55-873FF60DB8AF/08940886.2017.1338410.FP.PNG.

[24] N. Benseny-Cases, E. Álvarez-Marimon, H. Castillo-Michel, M. Cotte, C. Falcon, J. Cladera, Synchrotron-based fourier transform infrared microspectroscopy (μFTIR) study on the effect of alzheimer's aβ amorphous and fibrillar aggregates on PC12 cells, Anal. Chem. 90 (4) (Feb. 2018) 2772–2779, https://doi.org/10.1021/ACS.ANALCHEM.7B04818.

[25] D.P. Nualart, F. Dann, R. Oyarzún-Salazar, F.J. Morera, L. Vargas-Chacoff, Immune transcriptional response in head kidney primary cell cultures isolated from the three most important species in Chilean salmonids aquaculture, Biology 12 (2023) 924, https://doi.org/10.3390/BIOLOGY12070924, 12, no. 7, p. 924, Jun. 2023.

[26] J. Seras-Franzoso, A. Sánchez-Chardi, E. Garcia-Fruitós, E. Vázquez, A. Villaverde, Cellular uptake and intracellular fate of protein releasing bacterial amyloids in mammalian cells, Soft Matter 12 (14) (Mar. 2016) 3451–3460, https://doi.org/10.1039/C5SM02930A.

[27] K.J. Livak, T.D. Schmittgen, Analysis of relative gene expression data using real-time quantitative PCR and the 2(-Delta Delta C(T)) Method, Methods 25 (4) (2001) 402–408, https://doi.org/10.1006/METH.2001.1262.

[28] M. Le Berre, A. M.-B. de l'Office I. des, and undefined, Identification sérologique des rhabdovirus des salmonidés, agris.fao.org, 1977 [Online]. Available: https://agris.fao.org/search/en/providers/123819/records/64736041e17b74d2225320fc. (Accessed 3 February 2025).

[29] J. Winton, W. Batts, P. deKinkelin, M. LeBerre, M. Bremont, N. Fijan, Current lineages of the epithelioma papulosum cyprini (EPC) cell line are contaminated with fathead minnow, Pimephales promelas, cells, J. Fish. Dis. 33 (8) (Aug. 2010) 701–704, https://doi.org/10.1111/J.1365-2761.2010.01165.X.

[30] P. Garcia-Valtanen, et al., Autophagy-inducing peptides from mammalian VSV and fish VHSV rhabdoviral G glycoproteins (G) as models for the development of new therapeutic molecules, Autophagy 10 (9) (Sep. 2014) 1666–1680, https://doi.org/10.4161/auto.29557.

[31] D. Deluca, M. Wilson, G.W. Warr, Lymphocyte heterogeneity in the trout, Salmo gairdneri, defined with monoclonal antibodies to IgM, Eur. J. Immunol. 13 (7) (1983) 546–551, https://doi.org/10.1002/EJI.1830130706.

[32] M. Fernandez-Alonso, et al., Mapping of linear antibody epitopes of the glycoprotein of VHSV, a salmonid rhabdovirus, Dis. Aquat. Org. 34 (3) (1998) 167–176, https://doi.org/10.3354/DAO034167.

[33] G. Lorenzo, A. Estepa, J.M. Coll, Fast neutralization/immunoperoxidase assay for viral haemorrhagic septicaemia with anti-nucleoprotein monoclonal antibody, J. Virol Methods 58 (1–2) (Apr. 1996) 1–6, https://doi.org/10.1016/0166-0934(95)01972-3.

[34] F. Sanz, B. Basurco, M. Babin, J. Dominguez, J.M. Coll, Monoclonal antibodies against the structural proteins of viral haemorrhagic septicaemia virus isolates, J. Fish. Dis. 16 (1) (Jan. 1993) 53–63, https://doi.org/10.1111/J.1365-2761.1993.TB00847.X.

[35] J. Schindelin, et al., Fiji: an open-source platform for biological-image analysis, Nat. Methods 9 (7) (2012) 676–682, https://doi.org/10.1038/nmeth.2019. Jun. 2012.

[36] M. Yu, S.J. Levine, Toll-like receptor, RIG-I-like receptors and the NLRP3 inflammasome: key modulators of innate immune responses to double-stranded RNA viruses, Cytokine Growth Factor Rev. 22 (2) (Apr. 2011) 63–72, https://doi.org/10.1016/J.CYTOGFR.2011.02.001.

[37] T. Kawai, S. Akira, Toll-like receptors and their crosstalk with other innate receptors in infection and immunity, Immunity 34 (5) (May 2011) 637–650, https://doi.org/10.1016/J.IMMUNI.2011.05.006.

[38] N.J. Pillon, C.O. Soulage, N.J. Pillon, C.O. Soulage, Lipid peroxidation by-products and the metabolic syndrome, Lipid Peroxidation (Aug. 2012), https://doi.org/10.5772/46019.

[39] V. Chico, et al., Pepscan mapping of viral hemorrhagic septicemia virus glycoprotein G major lineal determinants implicated in triggering host cell antiviral responses mediated by type I interferon, J. Virol. 84 (14) (Jul. 2010) 7140, https://doi.org/10.1128/JVI.00023-10.

[40] M.V. Céspedes, et al., Engineering secretory amyloids for remote and highly selective destruction of metastatic foci, Adv. Mater. 32 (7) (Feb. 2020), https://doi.org/10.1002/ADMA.201907348.

[41] R. Thwaite, et al., Nanostructured recombinant protein particles raise specific antibodies against the nodavirus NNV coat protein in sole, Fish Shellfish Immunol. 99 (Apr. 2020) 578–586, https://doi.org/10.1016/j.fsi.2020.02.029.

[42] R. Gonzalez, P. Matsiota, C. Torchy, P. De Kinkelin, and S. Avrameas, "Natural anti-TNP antibodies from rainbow trout interfere with viral infection in vitro,", Res. Immunol. 140 (7) (Jan. 1989) 675–684, https://doi.org/10.1016/0923-2494(89)90021-7.

[43] A.S. Kolaskar, P.C. Tongaonkar, A semi-empirical method for prediction of antigenic determinants on protein antigens, FEBS Lett. 276 (1–2) (Dec. 1990) 172–174, https://doi.org/10.1016/0014-5793(90)80535-Q.

[44] S. Martinez-Alonso, A. Martinez-Lopez, A. Estepa, A. Cuesta, C. Tafalla, The introduction of multi-copy CpG motifs into an antiviral DNA vaccine strongly up-regulates its immunogenicity in fish, Vaccine 29 (6) (Feb. 2011) 1289–1296, https://doi.org/10.1016/J.VACCINE.2010.11.073.